Materials Chemistry and Physics 258 (2021) 123851

Contents lists available at ScienceDirect

Materials Chemistry and Physics

journal homepage: www.elsevier.com/locate/matchemphys

Surface oxidized/silanized graphite nanoplatelets for reinforcing an epoxy matrix

Nazrul Islam Khan [a,b], Sudipta Halder [a,c,d,*], Nabajyoti Talukdar [a], Subhankar Das [a,e], M. S. Goyat [f]

[a] Department of Mechanical Engineering, National Institute of Technology Silchar, Silchar, 788010, Assam, India
[b] Department of Mechanical Engineering, GMRIT, Rajam, Srikakulam, 532001, Andhra Pradesh, India
[c] Alabama Transportation Institute, The University of Alabama, Tuscaloosa, AL, 35487, USA
[d] Aerospace Engineering and Mechanics, Center for Advanced Vehicle Technologies, The University of Alabama, Tuscaloosa, AL, 35487, USA
[e] Department of Mechanical Engineering, Siddharth Institute of Engineering and Technology, Puttur, India
[f] Department of Applied Science, School of Engineering, University of Petroleum and Energy Studies, Dehrdaun, 248007, India

HIGHLIGHTS

- An industrially favorable two-step process for exfoliation of graphene sheets of GNPs.
- The importance of oxidation time and amine-functionalization of GNPs.
- Development of economical and advanced GNP/epoxy nanocomposites.
- Storage modulus of the GNPs/epoxy composites was increased to ~176% compared to baseline.
- Tensile strength, modulus and fracture toughness enhanced by ~98%, ~143% and ~53%.

GRAPHICAL ABSTRACT

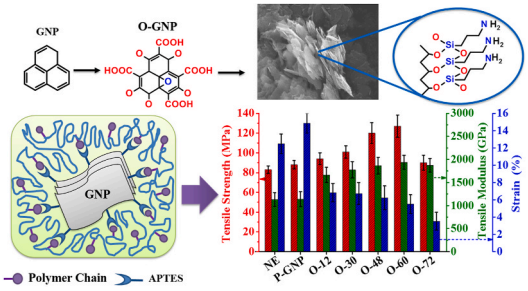

ARTICLE INFO

Keywords:
Graphene
Oxidation
Silanization
Thermo-mechanical properties
Mechanical properties

ABSTRACT

A simplistic and economical process was employed for the oxidation of graphite nanoplatelets (GNPs) using concentrated HNO_3, followed by their surface modification by amine functionalization via silanization with 3-aminopropyltriethoxysilane (APTES). The impact of the oxidation time of the GNPs (varied from 12 h to 72 h) and their surface functionalization was studied with respect to the change in thermo-mechanical and mechanical properties of the GNPs/epoxy nanocomposites. The degree of oxidation and functionalization of the GNPs was characterized using field emission scanning electron microscope (FESEM), Raman spectroscopy, Fourier transform infrared spectroscopy (FTIR), and thermo-gravimetric analysis (TGA). The optimized oxidation time (60 h) and surface functionalization of the GNPs resulted in the significant improvement in the storage modulus (~176%), glass transition temperature (T_g) (~15 °C), tensile strength (~98.71%) and tensile modulus (~142.66%) of the GNPs/epoxy nanocomposites as compared the to neat epoxy (NE) system. Such tremendous enhancement in the material properties by a facile and economical approach can exhibit an inordinate potential to replace the costly multistep oxidation methods of fabrication of graphene/epoxy nanocomposites at industrial scale.

* Corresponding author. Department of Mechanical Engineering, National Institute of Technology Silchar, Silchar, 788010, Assam, India.
E-mail addresses: shalder@mech.nits.ac.in, shalder@ua.edu (S. Halder).

https://doi.org/10.1016/j.matchemphys.2020.123851
Received 24 May 2020; Received in revised form 17 September 2020; Accepted 18 September 2020
Available online 22 September 2020

1. Introduction

Graphene (G) is made of single atom thick sheet of carbon atoms, which are sp^2 hybridized in nature and usually obtained from bulk graphite using top-down and bottom-up synthesis approaches. The G has been attracting the worldwide research community since its inception way back in 2004 [1,2]. The G, especially when exfoliated in the form of almost single layers possesses outstanding mechanical, electrical and thermal properties [3–7]. Lack of economical methods and complexities associated with the production of mass scale and fully exfoliated G restrict its use in various applications [8]. However, the G can be easily replaced with an alternate economical material such as graphite nanoplatelets (GNPs) that usually have square-shaped platelets with lateral dimensions on the micrometre scale and thicknesses on the nanometre scale less than 200 nm. The GNPs can be synthesized in mass-scale from bulk graphite through a simple chemical route [9]. The GNPs are used as second phase nanofillers to improve an epoxy matrix property owing to their excellent thermal, electrical and mechanical properties. However, non-exfoliated GNPs tend to form agglomerates in the viscous polymer matrices due to their large specific surface area and the presence of strong van der Waals forces [10]. Besides, if the aggregated GNPs are treated cost-effectively to exfoliate up to a certain level, it can replace single-layer G for their potential use in the fabrication of epoxy nanocomposites. To harness the best performance of the resulting nanocomposites, uniform dispersion and good interfacial bonding has to be ensured between the GNPs and the polymer matrix as carbon-based nano-fillers (CBN) have chemical inertness and poor wettability with most of the polymeric matrices [11,12].

Over the past decades, many researchers tried various surface functionalization techniques for improving the dispersion and interfacial adhesion of G with the polymer matrix [13–18]. In particular, different kinds of poly-siloxanes, including silane coupling agents, are frequently used to modify the graphene sheets [19–23]. The numerous functional groups of silane molecules such as amine, ethylene, epoxy, etc. can be attached on to the surface of the nanofiller that can further react with the polymer matrix to improve the overall performance of the resulted nanocomposites [24–29]. Currently, limited reports demonstrated a significant enhancement in the thermal and mechanical properties of graphene oxide (GO) synthesized via step-wise modification of graphite flakes using Hammer's, modified Hammer's and Staudenmaier's methods and followed by their silanization [20,30,31]. Ya Ni et al. [32] reported 120.9% enhancement in tensile strength (141 MPa) after the modification of graphite flakes through modified Hummer's method followed by grafting with poly(amidoamine). Most of the reported functionalization processes of graphene are based on a multistep process that adds up additional cost and time and acts as a barrier to industrialization. However, the oxidation of graphene by HNO_3 is a single step oxidation process to activate the graphene, which can be easily surface-functionalized using an amine or epoxy group [28,33,34]. Nevertheless, the oxidation time may exhibit a significant impact on the morphological and structural properties of the oxidized GNPs, which is not investigated in detail. The oxidation of the GNPs not only facilitates attachment of different functional groups like carboxylic acid, hydroxyl group, the epoxy group on their surface but also helps in de-agglomeration of the graphene stacking and make it accessible for silanization to occur through exfoliation. Al Saleh et al. investigated the effect of maleic anhydride grafting of GNPs on mechanical and thermal properties of polypropylene nanocomposites and reported that loading GNP 1 wt% to 5 wt% can significantly improve the mechanical performace and thermal stability [35]. Li et al. reported on acid intercalation and organosilane functionalization of GNP and showed significant improvement of damping and static dissipation capability of polyetherimide based composites [36]. Zhang et al. investigated the effect of silanization of GNPs with APTES on mechanical and thermal properties of silicon rubber composites and found ~38% improvement in tensile strength of the composites [37]. Thus, from literature it has been observed that functionalization of GNP through a facile process may be an cost effective approach for improvement of mechanical properties, thermal properties, damping capacity and static dissipation characteristics of epoxy based nanocomposites.

In our previously reported work, we have investigated the effect of oxidation and APTES post-functionalization of GNPs on the mechanical properties of carbon fiber reinforced polyer (CFRP) composites [38]. The tremendous improve in-plane and out-plane mechanical properties of the resulted CFRP composites proved that exfoliation and activation of GNPs through this cost effective method can be an effective method for their industrial application. A detailed investigation of the effect of the degree of functionalization on the thermo-mechanical and mechanical properties of GNPs/epoxy nanocomposites is not explored yet. In view of the above context, in this work, we have oxidized GNPs with HNO_3 from low oxidation time of 12 h to high oxidation time of 72 h to exfoliate up to a certain level and then silanized with 3-aminopropyltriethoxysilane (APTES) to attach amine functional groups on their surface. The degree of oxidation and functionalization of the GNPs are characterized in detail. The impact of the oxidation time and the surface functionalization of the GNPs are studied with respect to the change in thermo-mechanical and mechanical properties of the GNPs/epoxy nanocomposites.

2. Experimental section

2.1. Materials

GNPs of thickness 100–600 nm, lateral dimension varying from 1 to 100 μm, specific surface area >250 m^2/g and with a purity of 99.5% were purchased from Nanoshell, Intelligence Material Private Limited, UK. The concentrated HNO_3 (95%) and toluene of reagent grade supplied by AB Chemicals Private Limited. India. 3-aminopropyltriethoxysilane (APTES) with 99% purity was purchased from Alfa Aesar, India. An epoxy resin (Araldite, LY 556), hardener (HY906) and accelerator (DY070) were provided by Atul India Limited, India.

2.2. Surface modification of pristine GNPs

The surface functionalization of the GNPs has been discussed in details in our previously reported work [38,39]. The surface modification of GNPs was carried out in two steps, namely (1) oxidation and (2) silanization illustrated schematically in Fig. 1. Initially, pristine GNPs (P-GNPs) were oxidized with concentrated HNO_3 in an oxidation flux and continuously stirred by a magnetic stirrer at 1200 rpm in a heated oil bath (constant temperature 80 °C) for different periods such as 12 h, 30 h, 48 h, 60 h and 72 h to obtain different sets of the solution. Later on, the different sets of the solution were diluted and washed in a filter paper with double distilled water several times to maintain the pH of the solution at ~7 followed by further washing with ethanol and acetone. Then, the different sets of the samples were dried in vacuum at 70 °C for 12 h to obtain oxidized GNPs (O-GNPs). In the next step, all the sets of the 0.3 g O-GNPs were mixed with 20 mL toluene in round bottom flasks separately, and 1 wt% of APTES (with respect to filler weight) was mixed with 5 mL of toluene in separate beakers and was added dropwise to each O-GNPs solution. The addition of APTES to O-GNPs was carried out in a sonication bath at an amplitude of 90% for 10 min to properly mix the APTES solution to the O-GNP solution. The sonicated solution was refluxed at 110 °C using magnetic starring at 1200 rpm for 8 h. Then, the silanized GNPs (SO-GNPs) solution was filtered and washed several times with double distilled water, ethanol and acetone, respectively. Finally, the SO-GNPs were dried in a vacuum at 70 °C for 12 h.

2.3. Preparation of graphene filled epoxy nanocomposites

To investigate the effect of oxidation time and silanization of GNPs, epoxy nanocomposites were prepared by reinforcing with 0.5 wt% of P-

GNPs, O-GNPs and SO-GNPs separately and the properties were compared with that of the NE. The fabrication of GNPs reinforced epoxy nanocomposites is schematically illustrated in Fig. 2. Initially, 0.5 wt% nanofillers with respect to epoxy resin were added to the hardener and subjected to high energy acoustic cavitation under an ultrasonic liquid processor (Q700, Qsonica, USA) with a maximum output power of 700 W at a constant frequency of 20 kHz and amplitude of 70%. The temperature of the blend was continuously monitored and maintained below 40 °C to avoid degradation of the hardener using a chilled water bath. The ultrasonication pulse-on and pulse-off time were fixed at 10 s and 30 s, respectively. Mechanically agitation using a magnetic stirrer was simultaneously performed with the ultrasonication to avoid localized heating of the blend near the ultrasonic probe. Epoxy resin and accelerator were added to the blend of GNPs and hardener in a predecided ratio (epoxy: hardener: accelerator: 100: 95: 2). Then the resulting mixture was mechanically stirred using an impeller at 2000 rpm for 15 min. Finally, the mixture was degassed for 1 h to remove the entrapped air bubbles. The epoxy resin system was transferred to silicon molds and cured in a hot air oven at 120 °C for 2 h, followed by post-curing at 160 °C for 8 h.

2.4. Determination of oxidation degree of O-GNPs

The degree of oxidation with HNO_3 and the amount of carboxylic acid (COOH) group attached to GNPs was estimated using Marshall et al. [40] and Hu et al. [41] methods. O-GNPs were functionalized with DDA following the same procedure as described in our previously reported work [42]. For the calculation of the degree of oxidation, the weight measurements were carried out very carefully. About 40 mg of each set of the oxidized GNPs were added to 2 g of DDA. Then each set was subjected to sonication for 1 h at 70 °C. The sonicated sets were subjected to a high-speed magnetic stirring for 72 h at 110 °C. Later on, all the sets were cooled to room temperature and blended with 300 mL of ethanol for further sonication for 0.5 h followed by filtration with 0.45 μm PTFE filter paper of known weight and washed with ethanol. The filter cakes were dried in vacuum at 80 °C for 24 h and the final weight of filter cakes including filter paper was measured again and the change in weight was recorded.

2.5. Characterization

The Raman spectra of P-GNPs, O-GNPs and SO-GNPs were obtained from Laser Micro Raman System (Horiba Jobin Vyon, Model LabRam HR) with a resolution of 2 cm^{-1} using an Nd: YAG laser source. The laser source of 633 nm wavelength with 10 s integration time was used for recording the Raman spectra of the GNP samples and minimum 3 spectra were recorded for each sample. FTIR (Bruker Vertex 80 spectrometer, Germany) spectra of modified GNPs were recorded from 400 to 4000 cm^{-1} with a resolution of 0.2 cm^{-1}. For the FTIR analysis, the samples were first grounded to a very fine powder using mortar and pestle and mixed with potassium bromide (KBr 99.99% purity) powder and finally converted to transparent thin films. XRD patterns for GNPs before and after oxidation were recorded on X'pert Pro diffractometer (Phillips, PANalytical, Holland) using Cu Kα radiation source (λ = 1.540 Å) for each interval of 0.02° ranging from 5° to 90°. Morphological investigation of the GNPs and fracture surface analysis of GNPs/epoxy nanocomposites were performed FESEM (Zeiss, Supra 55VP microscope) at an acceleration voltage of 5 kV. The thermal characterization of GNPs and the nanocomposites were investigated with a TGA (NETZSCH STA 449F3 system, Germany) at a heating rate of 10 °C/min from room temperature to 800 °C in a nitrogen atmosphere. The thermo-mechanical behaviour of the nanocomposites was studied using a dynamic mechanical analyzer (DMA 8000 PerkinElmer system, U.S.A) under a single cantilever mode for specimens with a dimension of 25 × 8 × 2 mm^3 at an oscillation frequency of 1 Hz. The data was collected from room temperature to 120 °C at a scanning rate of 2 °C/min. The tensile and fracture properties of the nanocomposites were investigated according to American Society for Testing and Materials, ASTM D-638 standard with dimension 165 × 10 × 7 mm^3 and ASTM D-5045 standard with 40 × 10 × 4 mm^3 respectively using a computerized universal tensile machine (INSTRON, Model 5969) at a cross-head speed of 1 mm/min with a load cell of 50 kN.

3. Results and discussion

3.1. Morphological and structural characterization of GNPs

The morphologies of the P-GNPs and O-GNPs oxidized at different oxidation times 12 h, 30 h, 48 h, 60 h and 72 h designated as O-12, O-30, O-48, O-60 and O-72 respectively are shown in Fig. 3. The high magnification FESEM images of O-48, O-60 and O-72 are also reported discussed in our recently published work [38].

From Fig. 3(a), a clear indication of agglomerated graphene sheets of P-GNPs can be observed. Due to oxidation for 12 and 30 h, no significant morphological change was found for O-12 and O-30 (Fig. 3(b and c)). However, after oxidation for time beyond 30 h, exfoliation in the transverse direction, as well as the lateral separation of the graphene sheets, take place, which is found distinct in the O-48 and O-60 samples (Fig. 3(d) and (e)). In the case of O-60 (Fig. 3(e), a significant level of exfoliation of graphene sheets can be visible due to oxidation for 60 h. With the increase in oxidation time (O-72), no significant morphological change was observed and re-agglomeration occurred after washing and drying due to their high specific surface energy (Fig. 3(f)). From the morphological change, it can be inferred that oxidation of GNPs with HNO_3 for a minimum of 60 h can result in successful exfoliation of graphene layers due to effective attachment of various oxygenated groups on their surface. A positive impact of silanization on morphological change of GNPs is observed, as reported in our previous work [38]. Due to the attachment of highly active hydrophilic ligands (siloxane groups) onto GNPs, agglomerations of GNPs were reduced and some individual separated graphene layers can be observed for O-60. However, for O-72, due to exfoliation of graphene sheets as well as the lateral breaking of the GNP have formed some step-like pattern, which is found agglomerated after washing and drying. The lateral breaking with step patter formation and agglomeration at higher oxidation time has been explained in detail from AFM and FESEM analysis in our previously published work [38]. In case of GNPs oxidized for 72 h, a non-uniform layer thickness was found from the AFM analysis showing the few

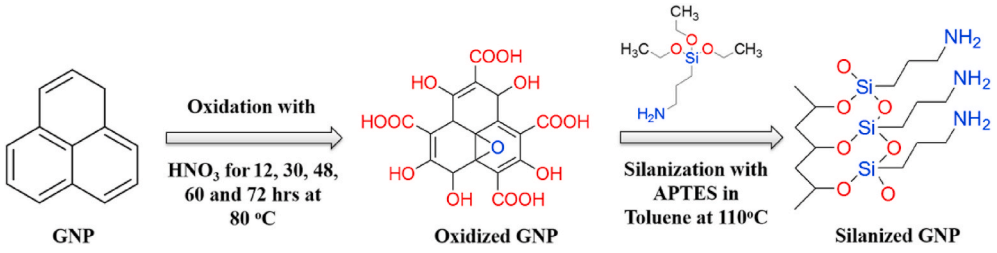

Fig. 1. Schematic illustration of the oxidation and surface functionalization of GNPs.

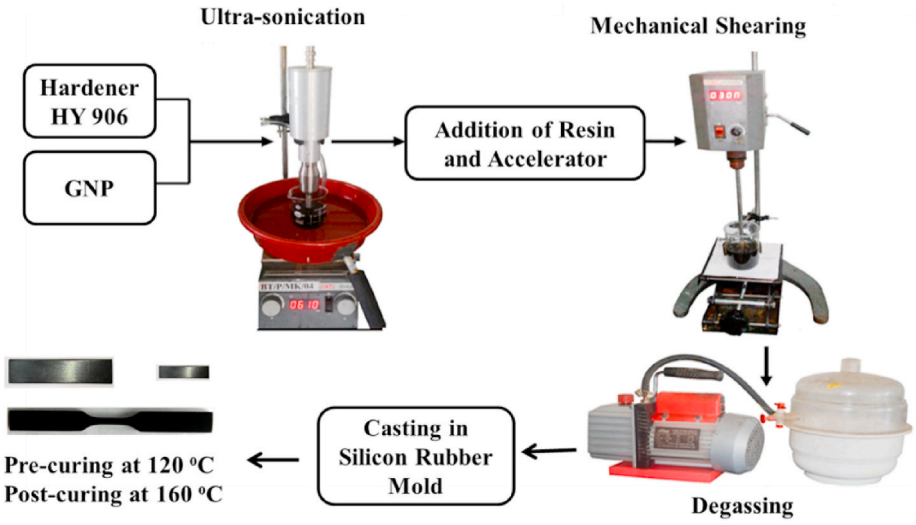

Fig. 2. Schematic illustration of the preparation of surface-functionalized GNP reinforced nanocomposites.

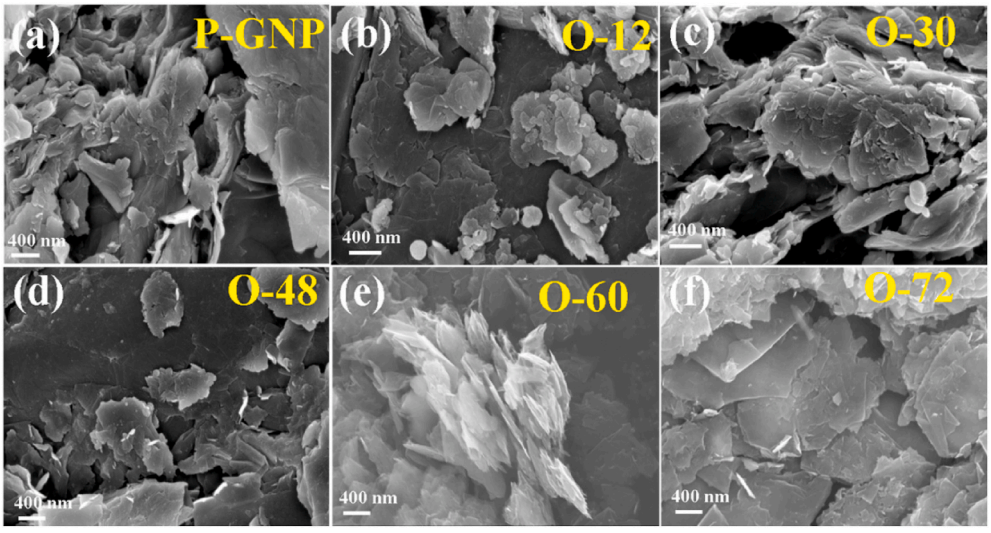

Fig. 3. FESEM images of (a) P-GNP, (b) O-12, (c) O-30, (d) O-48, (e) O-60, and (f) O-72.

successive steps of thickness ~2 nm, ~6.1 nm and ~9.2 nm. The generation of high surface energy due to extensive structural damage of GNPs resulted in re-agglomeration after washing and drying. Higher the de-agglomeration and separation of the thin graphene layers, the higher the dispersion in the epoxy matrix can be expected, which may further enhance the thermal and mechanical performance of the resulting nanocomposites.

3.2. Calculation of degree of oxidation from DDA functionalized GNPs

The acidic functional groups (COOH) attached on the surface and edges of O-GNPs react with DDA to form GNP-DDA zwitterion [40]. For every COOH group attached to GNPs, there will be one DDA molecule added to it. The variation of increase in mass percentage with the oxidation time is shown in Fig. 4.

It can be observed that due to the increase in oxidation time, there is a drastic change in mass percentage. The mass percentage increases significantly up to 60 h of oxidation (12.04%), and then a minor change in mass percentage (12.12%) value for 72 h of oxidation can be observed. Due to the formation of zwitterion, the weight of the samples after DDA treatment increases, which is a direct measure of the degree of oxidation. The increasing mass percentage indicates a higher degree of oxidation or attachment of more functional groups on the surface of GNPs. The amount of COOH group attached to GNPs increases up to 60 h of oxidation and a saturation level is reached on further increase in oxidation time.

3.3. Raman spectroscopic analysis

Raman spectroscopy provides an important characterization tool for carbon-based material by showing different spectra for sp, sp^2, sp^3 hybridized carbon. The Raman spectra of P-GNPs, O-GNPs and SO-GNPs are shown in Fig. 5(a) and (b). In the spectrum at the high-frequency zone, two distinct bands are observed showing the characteristics of the GNP. These bands are a graphitic band (G-band) at 1580 cm^{-1} and disorder or defect band (D-band) near about 1340 cm^{-1}. The ratio between the intensity of D-band and G-band, i.e., I_D/I_G is related to the degree of disorder on the P-GNPs. The defects on the surface of the P-GNPs are due to the attachment of different surface functional groups during the functionalization reaction stated above. As the I_D/I_G increases, the proportion of sp^3 carbon in the GNP increases, which directly gives the measure of the defect created on the P-GNPs. From

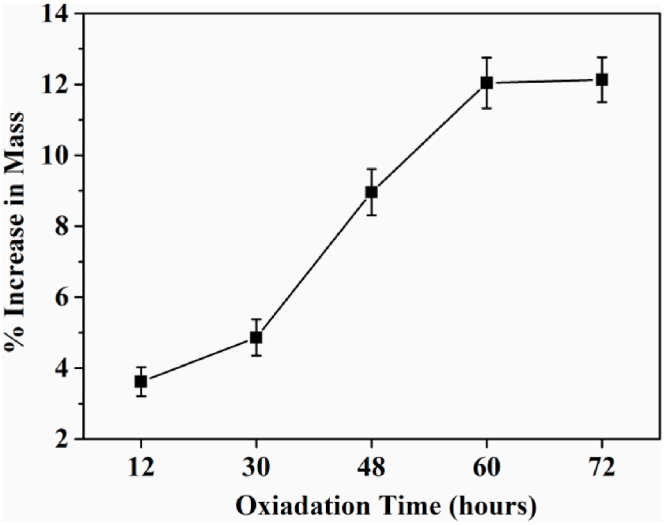

Fig. 4. Variation of degree of oxidation of GNP-DDA Zwitterion with oxidation time.

Fig. 5(c), the I_D/I_G value for P-GNP is 0.3568, i.e., there is a small amount of inherent defect in the pristine material which may be generated during their production. After oxidation, the I_D/I_G increases as the oxidation time is increased and reaches a maximum value of 0.6255 at 60 h of oxidation and then decreases on further increase in oxidation time. The oxidation of GNP breaks some of the double bonds in the hexagonal structure and thus increases the degree of disorder on the P-GNPs. Moreover, effective exfoliation as also observed from Fig. 3 after oxidation and silanization in case of O-60 resulted in maximum defect density. The decrease in I_D/I_G ratio at higher oxidation time (O-72) is due to the structural damage in the lateral direction of graphene sheets [39].

After silanization, due to the addition of functional groups on the defect sites, the degree of disorder on the GNPs are further increased and reached a maximum value of 1.0510 for SO-60 then follows the same trend as in case of O-GNPs (Fig. 5(d). The 2D band near about 2738 cm^{-1} from the Raman spectrum of functionalized graphitic nanofillers can be used for comparing the degree functionalization or amount of foreign materials doped with them [43]. The decrease in intensity and broadening of the 2D band with SO-60 justifies the highest degree of functionalization (Fig. 5(b)) [44]. From the FESEM image (Fig. 3), maximum de-agglomeration was observed at 60 h of oxidation followed by silanization, which is also an indication of maximum defects generation and effective surface functionalization. Thus we can conclude that 60 h of oxidation time incorporates the highest defect density, which in turn further helps in effective silanization to occur.

3.4. Molecular architecture of amine-functionalized GNPs

Infrared spectroscopy is an important technique for the identification and characterization of functional groups present in a compound. The FTIR spectra of P-GNP, O-GNP oxidized for 12 h and SO-GNPs with a variation of oxidation time are shown in Fig. 6.

In the case of P-GNPs, a broad peak at 3435 cm^{-1} can be observed which is mainly due to the hydroxyl groups of the moisture present. After oxidation for 12 h (O-12), the peak intensity is found increased due to the attachment of different oxygenated functional groups. Intense common peaks of modified GNPs at frequencies 1032, 1115, 1575, 1625, 3435 cm^{-1} are observed. However, there is variation in intensities

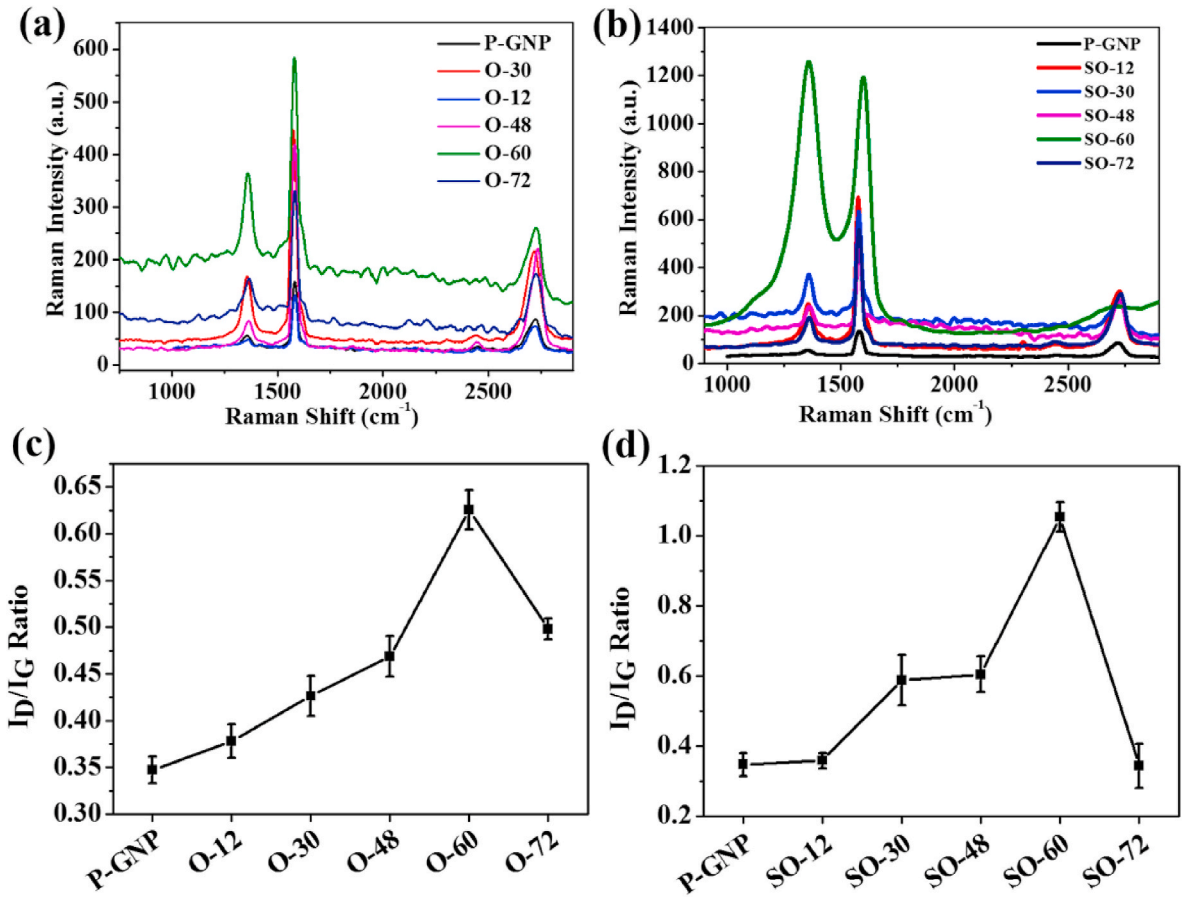

Fig. 5. Raman spectra of P-GNP along with (a) O-GNPs and (b) SO-GNPs. The variation of I_D/I_G ratio for (c) O-GNPs and (d) SO-GNPs.

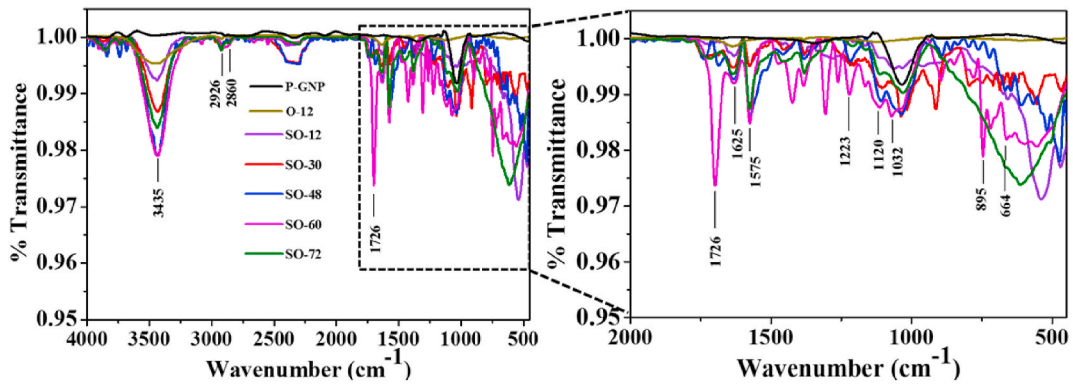

Fig. 6. FTIR spectra of P-GNP, O-12 and amine-functionalized GNPs oxidized for 12, 30, 48, 60 and 72 h.

of these vibration bands for different functionalization parameters suggesting a change in the degree of interaction amongst the modifying agent and GNPs [45]. The absorption spectra observed at 3435 cm^{-1} is corresponding to hydroxyl (-OH) groups coming from the atmospheric moisture and oxygenated groups attached to SO-GNPs. The intensity of this peak is found to increase after oxidation and silanization. These may be due to an increase in the number of hydroxyl groups attached to GNPs due to an increase in oxidation time. After oxidation, oxygenated functional groups are attached, which are the active sites for attachment of silane molecules through hydrolysis and condensation reaction. So, the higher the oxidation level, the higher is the chance to get silanized [37]. Other characteristic peaks observed at 2926 cm^{-1} and 2860 cm^{-1} are due to the presence of symmetric and asymmetric -CH_2 stretching coming from the silane polymer chain justifying successful silanization which is absent in case of P-GNPs. The evidence of -COOH group formation is demonstrated through the new peak generated for O-12 and SO-GNPs (1726 cm^{-1} and 1223 cm^{-1}) corresponding to the C=O and C-O stretching. Further confirmation is drawn through the presence of new bands at 1625 cm^{-1} and 1380 cm^{-1}, arising from intermediate oxidation products [46] and O–H bending vibration. The difference in spectra for amine-functionalized GNPs arises from the disappearance and appearance of various peaks. One such example is harvested from the appearance of a peak at 1575 cm^{-1} (primary NH_2 of APTES) and disappearance of peak at 1625 cm^{-1} (C=C stretching). The appearance of additional bands conjugated at frequencies 1120 cm^{-1} and 1032 cm^{-1} due to Si–O–Si stretching, 664 cm^{-1} due to Si-C, 895 cm^{-1} due to hydrolyzed silane, Si-OH were also found in the FTIR spectra [38]. In the case of SO-72, at higher oxidation time, attachment of excess hydroxyl groups are formed. These hydroxyl groups form bonds with the other functional groups and appear as a broad peak (merging of small characteristic peaks on broad peaks) at the lower wavenumber region. Uniform coverage of the silane moieties on the GNPs entrenches a better chance of covalent bonding between amine end groups of silane moieties and an epoxy group of the matrix system. Thus, we can expect better mechanical properties from the resulting nanocomposites. Thus FTIR analysis confirms the effective attachment of the siloxane group along with hydrophilic NH_2 onto GNPs.

The XRD patterns of GNPs before and after oxidation for 60 h are shown in Fig. 7. From the figure, it is observed that the peak appeared at a 2θ angle of 26.63° is corresponding to the graphitic structure of GNPs with Miller indices (002) [28,47]. This peak is common for both pristine and oxidized GNPs, indicating no structural change or conversion of graphite to graphene oxide (GO) has taken place. But the oxidation of GNP was confirmed from 1726 cm^{-1} and 1223 cm^{-1} bands corresponding to the C=O and C-O stretching in the FT-IR spectra, as shown in Fig. 6. The absence of graphene oxide characteristic peak at 2θ angle of nearby 11.05° in XRD spectra is mainly because of complete separation or exfoliation of individual graphene layers was not possible through single-step acid treatment [48]. Another interesting observation

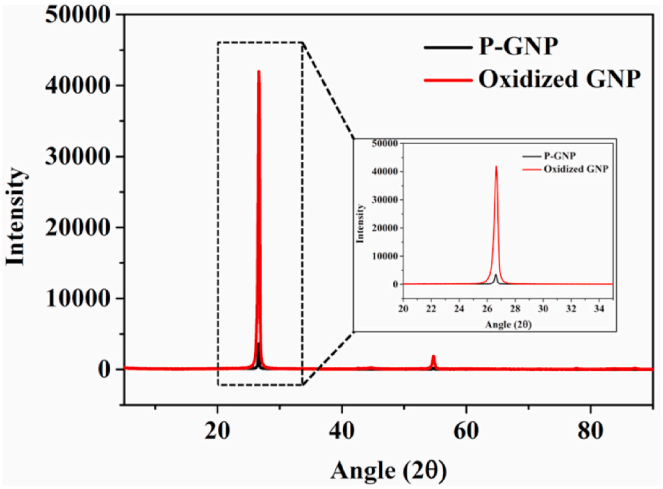

Fig. 7. XRD pattern of GNPs before and after oxidation with HNO_3.

is the intensity of the peak after oxidation has been significantly increased as compared to that of P-GNPs. After oxidation, the graphite structure of GNPs become prominent due to removal of bi-products and exfoliation of agglomerated 3D graphite layers. Thus, from the morphological, chemical and structural investigation, we can confirm the structure of GNPs as graphite oxide after the oxidation with HNO_3.

3.5. Thermo-gravimetric analysis of GNPs

TGA analysis was carried out to make sure the presence of different oxygenated and silane functional groups over the surface and edges of GNPs claimed by Raman and FT-IR analyses. Fig. 8(a) and (b) show the TGA plots of O-GNPs and SO-GNPs, respectively. In the case of O-GNP samples, as shown in Fig. 8(a), the degradation near about 100 °C is due to be the presence of moisture on the surface of the GNPs. The degradation of O-GNPs within the temperature range of 300–350 °C increases with an increase in oxidation time, and the lowest residual mass was obtained for the O-60 sample. This is due to the loss of more number of –OH and –COOH groups present on the surface and edges of GNPs. In the case of SO-GNP samples (Fig. 8(b)), the same trend has been observed like O-GNP, except for the weight loss here is slightly higher as compared to that of O-GNP samples. This might be because of the degradation of the reaction intermediates formed between oxygenated functional groups and APTES having higher molar mas as compared to the oxygenated functional groups. From TGA plots, it has been observed that the degradation is maximum in case of SO-60 sample within temperature range 550–650 °C followed by SO-48, SO-72, and SO-30 because of more pyrolysis of silane moieties present on the SO-60

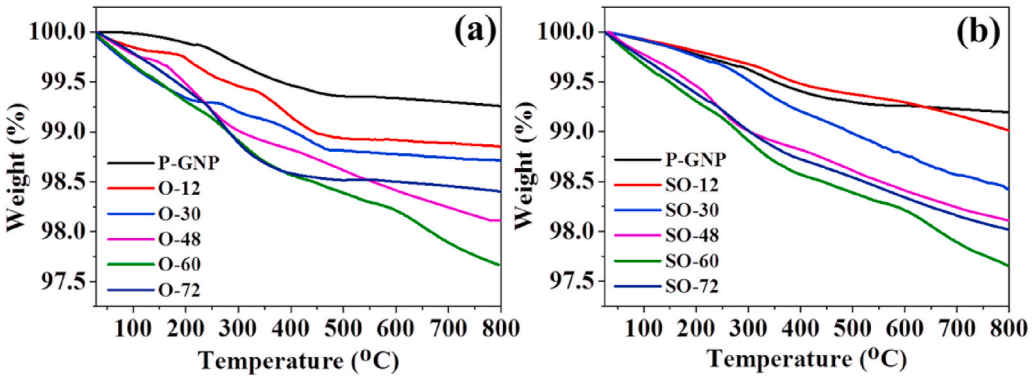

Fig. 8. Thermo-gravimetric analyses of (a) O-GNPs and (b) SO-GNPs along with P-GNPs.

sample as compared to the other indicating effective functionalization at 60 h of oxidation.

3.6. Thermo-mechanical and interfacial interaction of GNP/epoxy nanocomposites

Thermo-mechanical behaviour of the GNP/epoxy nanocomposites is studied by DMA under dynamic load and temperature. From the DMA analysis, the molecular relaxation behaviour, and the damping spectra of NE, as well as different SO-GNP reinforced nanocomposites are investigated to evaluate the polymer mobility, interfacial interaction on load transferability and segment confinement. The combined effect of oxidation time and silanization on the storage modulus, G′ (MPa) and damping factor, tan δ, is shown in Fig. 9. Fig. 9(a) evidences the significant variation of the storage modulus, G′ of neat epoxy resin reinforced with P-GNPs and SO-GNPs. At room temperature and glassy plateau (30 °C), the G′ for NE is ~518 MPa, which has been enhanced to almost 700 MPa with P-GNPs and a maximum value of 1430 MPa with SO-GNPs (SO-60). Hence, indicating a significant enhancement of G′ by almost ~36% and ~176% for P-GNP and SO-60, respectively, compared to NE.

The capability to restrict the molecular relaxation of the epoxy network and mobility of the oligomers at the interface by the incorporation of P-GNPs and SO-GNPs might be the reason behind the increase in storage modulus. Moreover, the incorporation of uniformly dispersed SO-GNPs having amine groups at the end might have created the conformational change of the polymer network near the vicinity of the GNPs, increasing storage modulus of the composites. On the other hand, the broadening of temperature window due to the incorporation of SO-GNPs corresponding to the degradation of G′ indicates the formation of high modulus interfaces between the silanized GNPs and the epoxy matrix and thus ameliorating the positive impact of silanization. Fig. 9 (b) depicts the significant changes in tan δ of the SO-GNP reinforced nanocomposites, and the peak of tan δ was used to determine glass transition temperature, T_g. The T_g for epoxy was increased from 143 °C to 158 °C due to addition GNPs oxidized for 60 h, followed by silanized. With the addition of P-GNPs, a minor increase in T_g value (148 °C) was observed, which was drastically increased up to 158 °C due to the addition of SO-GNPs. The drastic enhancement of T_g is due to the wrinkled structure and high specific surface area, effective restriction of chain mobility by SO-60 and the covalent bonding with SO-GNPs and polymer matrix [49]. For all the variation of oxidation time, the T_g values were near about the same, but for SO-72, a drastic decrease in T_g value (123 °C) can be observed. This may be due to the re-agglomeration of GNPs during processing and, thus, poor interaction with the matrix phase. The increase in the T_g value due to the addition of amine-functionalized GNPs in the epoxy suggests that strong interactions exist between GNPs and polymer networks.

For further verification of the nature of interfacial interaction between GNPs and polymer matrix, heat capacities of the nanocomposite were measured with differential scanning calorimetric (DSC) analysis and polymer cooperative length scales were calculated according to the method of Donth [50]. Cooperatively rearranging region (CRR) of nonhomogeneous glass is defined as the number of segments that can move for the network relaxation to occur upon a thermal fluctuation without changing its environment [51]. CRR is a structural unit of the polymer, which may be monomers, monomer segments, or even polymer chains. The CRR volume (ξ^3) at T_g is calculated using the following equation (1) [50]:

$$\xi^3 = \frac{k_B T_g^2 \Delta(1/c_v)}{\rho(\delta T)^2} \quad (1)$$

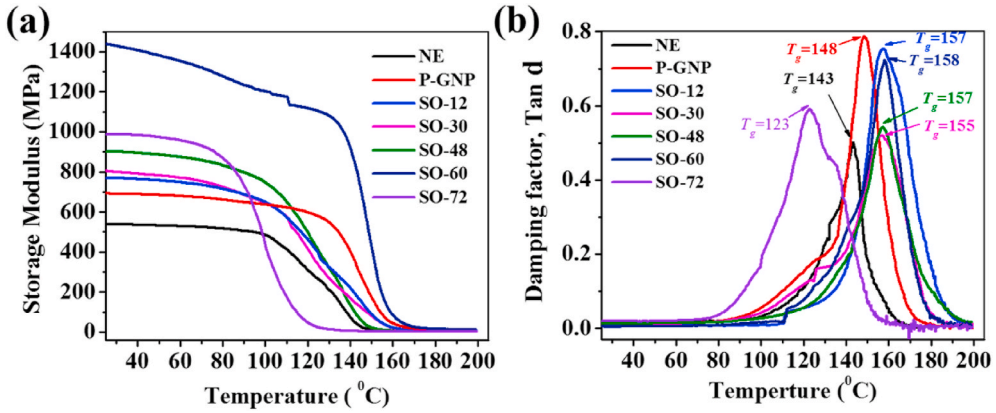

Fig. 9. (a) Dynamic mechanical analysis and (b) damping factor plots showing T_g of NE, P-GNPs and SO-GNP reinforced nanocomposites.

Where, k_B is Boltzmann constant, T_g is the glass transition temperature, C_v is heat capacity at constant volume, ρ is the density of the composite (1.21 g/cm^3) and δT is the mean temperature fluctuation at T_g. The C_v value is approximated from heat capacity at constant pressure, C_p obtained from DSC curve and δT is estimated using Donth's approach, in which $\delta T = \frac{\Delta T}{2.5}$ and ΔT is the temperature range over which C_p changes from 16% of $\Delta C_p(T_g)$ to 84% of $\Delta C_p(T_g)$. One example of calculating CRR from C_p vs. temperature plot and variation of CRR with the addition of functionalized GNPs are shown in Fig. 10(a) and (b).

The CRR value for neat epoxy was observed as ~1.3025 nm (Fig. 10 (b)), which was increased slightly due to the addition of P-GNPs (~1.41 nm). Moreover, due to the addition of SO-GNPs, with the increase in oxidation time, the CRR was increased to a maximum value of ~1.87 nm (SO-60) and then decreased on further increase in oxidation time. A minor variation of CRR was observed from the figure, which is mainly due to its dependency on a large extent on the amount of filler content, which was kept the same in all the cases (0.5 wt%). The CRR volume increases with an increase in flexibility of the percolating interphase due to the addition of SO-GNPs and the tan δ curve becomes narrower (Fig. 9 (b)). The larger CRR size of nanocomposites is attributed to covalent bonding between GNP and epoxy network, which restricts the mobility of the segments and helps in chain relaxation to occur [51]. In general, in the case of a neat epoxy system, the higher the crosslinking density, the lesser the CRR size due to the restriction of the polymer chain movement [52]. However, due to the incorporation of the uniformly distributed amine-functionalized GNPs, confinement of the polymer segment occurs and necessitates the coordinated movement of polymer chain for relaxation to occur, resulting in increased in size of CRR. Moreover, the increase in CRR size due to the addition of SO-GNP confirms a homogeneous cross-linking topology of the resulting epoxy nanocomposite [53]. Strong interfacial interaction between the siloxane chain of GNP and epoxy polymer chain will increase the activation energy barrier for the movement of the polymer chain thereby increasing T_g.

3.7. Mechanical properties of nanocomposites

To investigate the effect of GNPs oxidized for different oxidation time (12, 30, 48, 60, 72 h) followed by their silanization, tensile and fracture properties of the nanocomposites have been investigated according to ASTM standards. The representative stress vs. strain plots of the nanocomposites is shown in Fig. 11.

The variation of tensile strength, tensile modulus and percentage strain of SO-GNPs reinforced nanocomposites along with NE and P-GNPs are shown in Fig. 12(a) and (b), respectively and also listed in Table 1. The tensile strength for NE was observed as 83 MPa, which was enhanced up to 88 MPa (~6.02%) due to the addition of P-GNPs. The tensile strength was further improved due to the incorporation of O-GNPs. The enhancements of tensile strengths were about 13.25%, 21.68%, 44.58%, 53.01% and 8.43% for O-12, O-30, O-48, O-60 and O-72, respectively with respect to NE (Fig. 12(a)).

It can be observed that the tensile strength increases with an increase in oxidation time up to 60 h of oxidation (127 MPa) and then decreases on further increase in oxidation time. With the increase in oxidation time, the amount of oxygenated functional groups (Fig. 4) attached on the surface and edges of GNPs increases, which further helped in exfoliation of GNPs (Fig. 3) and better dispersion in the epoxy matrix. The decrease in tensile properties of the nanocomposites with the increase in oxidation time above 60 h is due to the agglomeration of laterally broken GNPs, as also observed from morphological investigation under FESEM (Fig. 3(e)).

Similarly, due to the addition of SO-GNPs, the tensile strength showed the same increasing trend but significantly higher than that of O-GNPs. The tensile strengths of SO-12, SO-30, SO-48, SO-60 and SO-72 are 116, 137, 151, 165 and 121 MPa respectively showing ~39.76%, 65.06%, 81.92%, 98.79%, and 45.78%, respectively enhancement with respect to NE and ~31.82%, 55.68%, 72.59%, 87.50%, and 37.50%, respectively with respect to O-GNPs reinforced nanocomposites (Fig. 12 (b)). Ni Y. et al. observed that the maximum tensile strength that can be achieved with graphene reinforced nanocomposites is ~141 MPa showing 120.9% enhancement as compared to the neat epoxy system [26]. But, in this paper, we have reported for the first time such a huge tensile strength enhancement up to 165 MPa, showing 98.79% enhancement compared to neat epoxy due to the addition of stepwise amine-functionalized GNPs. The outstanding improvement in tensile strength may be due to good dispersion of the exfoliated GNPs in the epoxy system [28]. The amine functional groups attached with GNPs form covalent bonding with epoxy ring present in the matrix system thereby improves the mechanical properties of nanocomposites through strong interfacial mechanical interaction between the filler and matrix system.

The variation of tensile modulus with the variation of oxidation time followed by silanization is also shown in Fig. 12(a) and (b). The tensile modulus of NE is ~1132 MPa, which got marginally enhanced to 1137 MPa due to the addition of P-GNPs. It is also found that the tensile modulus increases with an increase in oxidation time and reaches a maximum value of 1938 MPa at 60 h of oxidation and then decreases with a further increase in oxidation time. Moreover, by comparison, nanocomposites reinforced with oxidized followed by silanized GNPs show higher tensile modulus than that of O-GNPs. The maximum tensile modulus enhancement was ~142.66% (from 1132 to 2747 MPa) for SO-60 as compared to NE, and ~141.60% (from 1138 to 2747 MPa) as compared to P-GNP reinforced nanocomposites. All the enhancements due to the addition of SO-GNPs justify the ameliorating effect of amine-functionalized GNPs on the epoxy system. Maximum tensile strength and tensile modulus observed with SO-60 confirm structural stability,

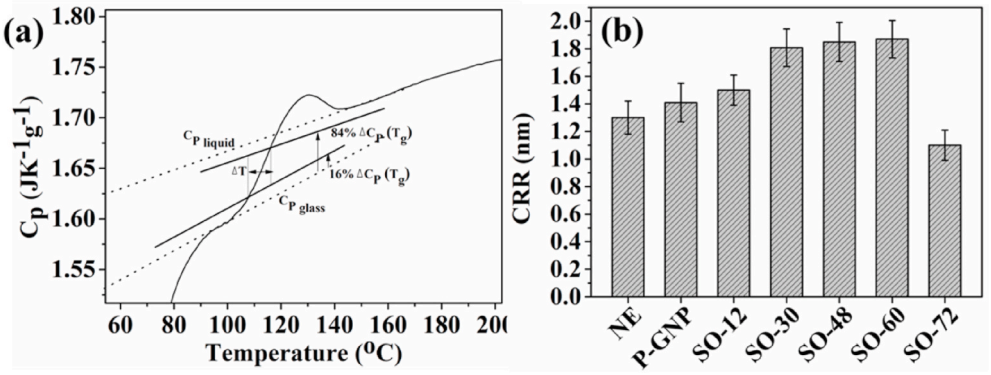

Fig. 10. (a) Typical example showing the procedure to calculate CRR from the C_p plots and (b) variation of CRR of the neat epoxy matrix due to the addition of P-GNPs and functionalized GNPs.

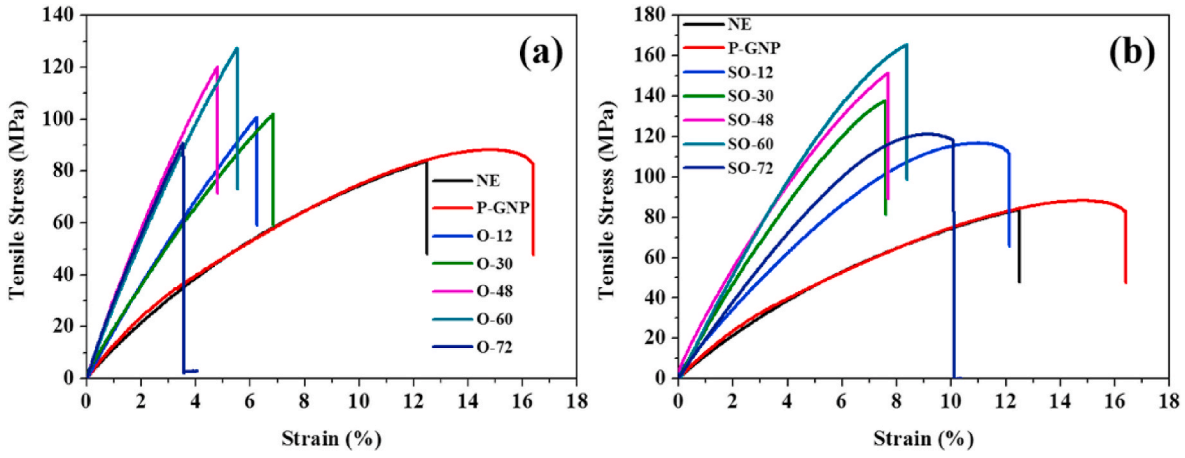

Fig. 11. The stress-strain plots of (a) O-GNPs and (b) SO-GNP based nanocomposites.

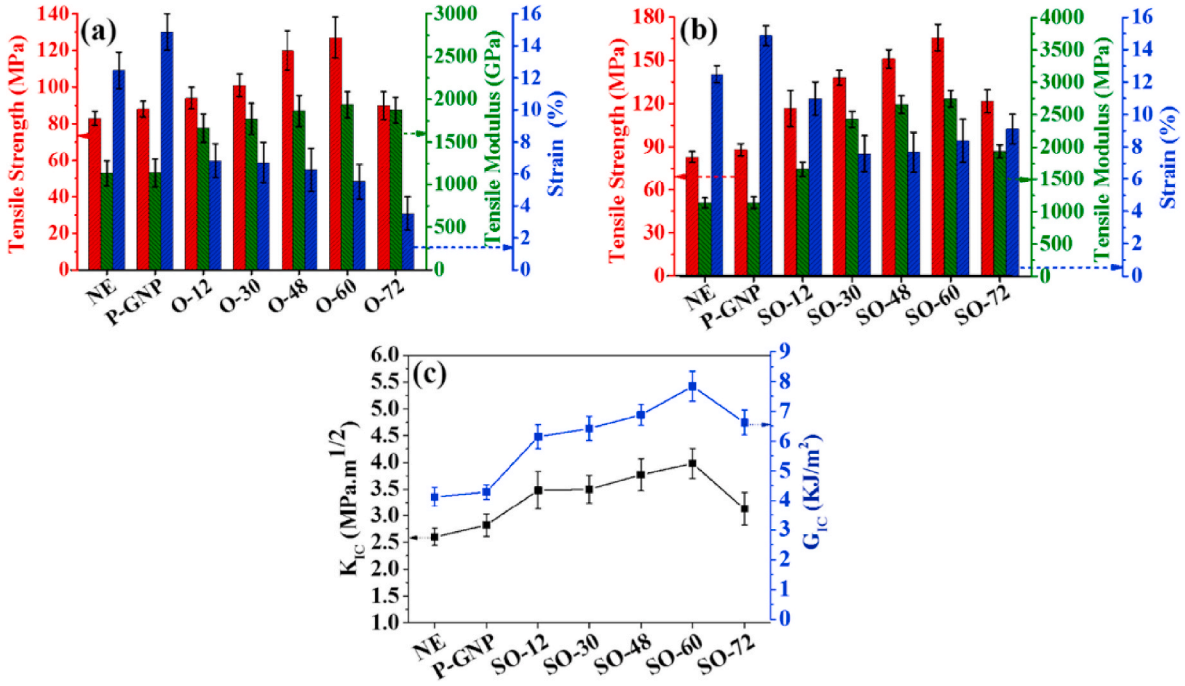

Fig. 12. Bar diagram showing variation tensile strength, percentage strain and Young's modulus of NE and P-GNP nanocomposites along with (a) O-GNPs and (b) SO-GNPs and (c) variation of K_{IC} and G_{IC} due to addition of SO-GNPs.

Table 1
Tensile properties of surface functionalized GNP reinforced nanocomposites.

Sample Code	Tens. Strength (MPa)	a (%)	b (%)	% Strain	a (%)	b (%)	Y. Modulus (MPa)	a (%)	b (%)
NE	83 ± 3.75	–	–	12.48 ± 0.52	–	–	1132 ± 80	–	–
P-GNP	88 ± 4.22	6.02	–	14.87 ± 0.60	19.15	–	1137 ± 90	0.44	–
O-12	94 ± 5.98	13.25	6.81	6.83 ± 1.06	−45.27	−54.06	1664 ± 166	46.99	46.35
O-30	101 ± 6.24	21.68	14.77	6.72 ± 1.27	−46.15	−54.80	1773 ± 179	56.62	55.93
O-48	120 ± 10.59	44.57	36.36	6.24 ± 1.36	−50	−58.03	1865 ± 180	64.75	64.02
O-60	127 ± 11.28	53.01	44.31	5.51 ± 1.08	−55.84	−62.94	1938 ± 150	71.20	70.44
O-72	90 ± 7.58	8.43	2.27	3.52 ± 1.04	−71.79	−76.32	1664 ± 146	46.99	46.35
SO-12	116 ± 12.56	40.59	31.82	10.99 ± 1.02	−11.93	−26.09	2433 ± 110	114.92	113.98
SO-30	137 ± 5.24	66	55.68	7.58 ± 1.11	−39.26	−49.02	2660 ± 120	134.98	133.94
SO-48	151 ± 6.39	81.92	72.59	7.68 ± 1.24	−38.46	−48.35	2747 ± 135	142.66	141.60
SO-60	165 ± 9.36	98.79	87.50	8.38 ± 1.33	−32.85	−43.64	1939 ± 128	71.28	70.53
SO-72	121 ± 7.82	45.78	37.50	9.12 ± 0.91	−26.92	−9	1664 ± 100	46.99	46.35

a: % enhancement with respect to NE and b: % enhancement with respect to P-GNP.

better dispersibility, and better interaction of GNPs with the epoxy system.

The variation of percentage strain with the variation of oxidation time followed by silanization is also shown in Fig. 12 (a) and (b). It can be observed that the percentage strain increases due to the addition of P-GNPs in the matrix and then decreases for the incorporation of oxidation GNPs. Higher oxidation time resulted in an increase in the level of exfoliation, which in turn might have restricted the polymer chain movement during loading absorbing more energy to get deformed and thus reducing percentage strain and enhancing Young's modulus. The surface moieties attached after stepwise functionalization enhanced the flexibility of the polymer chain. The enhancement of flexibility of the polymer chain increased percentage strain of the SO-GNP nanocomposites as compared to the O-GNPs.

Based on the above results, only amine-functionalized GNP reinforced nanocomposites were selected to investigate the effect of silanization on their fracture properties. Typically, the fracture toughness (K_{IC}) and fracture energy (G_{IC}) for anhydride based neat epoxy (NE) system are about 2.60 MPa $m^{1/2}$ and 4.12 kJ/m^2 respectively (Fig. 12 (c)). As expected, the K_{IC} and G_{IC} for the nanocomposites were increased with an increase in oxidation time followed by silanization as compared to P-GNPs (2.82 MPa $m^{1/2}$ and 4.29 kJ/m^2). Maximum K_{IC} and G_{IC} values were observed for SO-60 (3.975 MPa $m^{1/2}$ and 7.84 kJ/m^2), which showed ~53% and 90% improvement respectively compared to neat epoxy. Our investigation on Mode-I fracture toughness confers the ameliorating effect of silanization of GNPs on stiffness modulation by covalent bonding between SO-GNPs and epoxy matrix. Thus, from the results, it can be observed that the combination of oxidation time and amine functionalization also has significant effects on the fracture properties of the resulted nanocomposites.

3.8. Fracture surface analysis under FESEM

The fracture surfaces of the tensile test samples were examined under FESEM to compare the fracture mechanisms in neat epoxy as well as in nanocomposites reinforced with functionalized GNPs. The FESEM images of the fracture surfaces of NE, P-GNP, O-GNP and amine-functionalized GNP reinforced nanocomposites are depicted in Fig. 13 (a–d). The fracture surface of the neat epoxy system is smooth, with few rivers like patterns indicating brittle fracture (Fig. 13(a)). The fracture surface of P-GNP reinforced nanocomposites depicts some shear-yielding and out plane crack path diversion zones along with the formation of cavities. These may be due to the presence of P-GNP with poor interfacial adhesion with the epoxy matrix. With the addition of O-GNPs, the roughness of the fracture surface increased, which is a measure of high energy requirement before failure and good interfacial interaction between filler and matrix (Fig. 13(b)). Moreover, due to the addition of O-GNPs (Fig. 11(c)), some filler pull-out zones on the fracture surface are observed, indicating limited interfacial interaction with the epoxy matrix. Though uniformly dispersed and well-exfoliated O-GNPs enhanced the tensile strength of the epoxy system but poor filler-matrix interaction restricted further enhancement of the mechanical as well as thermal properties of the nanocomposites. Besides, due to the incorporation of SO-GNPs, strong interfacial adhesion between GNP and epoxy matrix can be observed from Fig. 13(c). This is mainly due to strong covalent bond formation between SO-GNPs and the epoxy matrix. Thus, the fracture surface also revealed the ability of stepwise surface functionalization of GNPs through oxidation followed by silanization on the increment of tensile and fracture properties of the nanocomposites.

4. Conclusions

An industrially favorable two-step process was successfully employed for the exfoliation of graphite nanoplatelets (GNPs). An optimized oxidation time of 60 h followed by the amine-functionalization of GNPs, significantly improved thermo-mechanical and mechanical properties of the GNPs/epoxy nanocomposites. The effect of functionalization procedure on exfoliation of GNPs have been confirmed from FESEM analysis and showed that 60 h of oxidation followed by silanization results in best exfoliation level with good stability. The change in chemical state investigated from FTIR and Raman analysis showed that with increase in oxidation time, effective

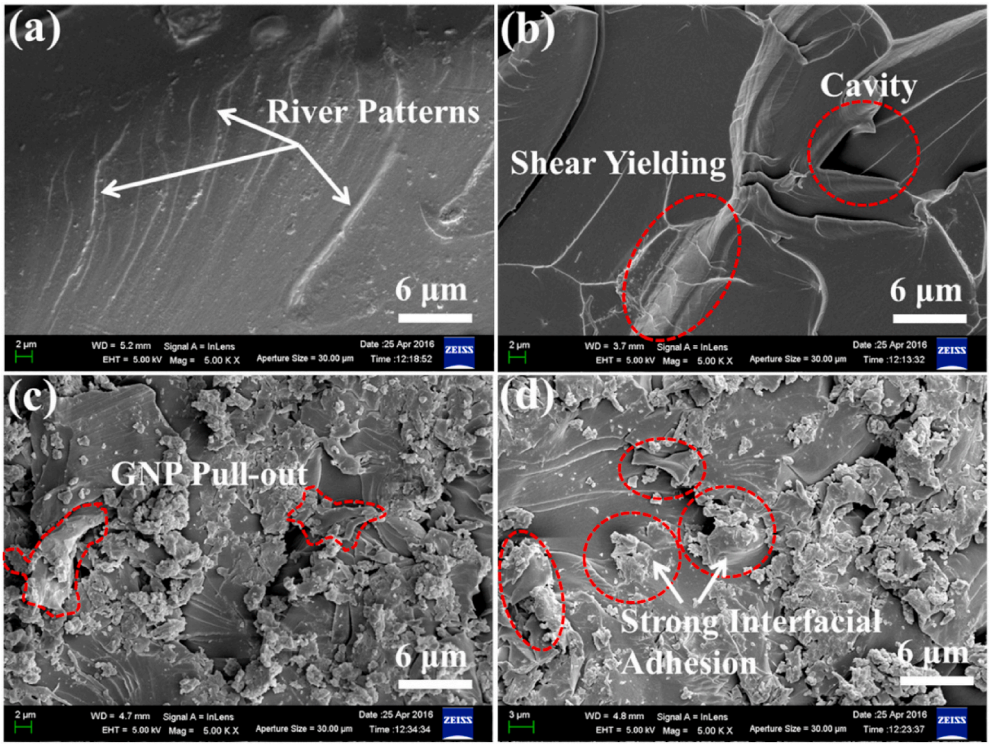

Fig. 13. FESEM images of fracture surfaces of (a) NE, (b) P-GNPs, (c) O-60 and (d) SO-60.

functionalization is possible through the reaction between active sites of oxidized GNPs and the silane moieties. The effect of the functionalized and exfoliated GNPs on the performance improvent of epoxy nanocomposites were confirmed from their thermal and mechanical property investigation. The modified GNPs resulted in the significant improvement in the storage modulus (~176%), glass transition temperature (T_g) (~15 °C), tensile strength (~98.71%) and tensile modulus (~142.66%) of the GNPs/epoxy nanocomposites compared to neat epoxy (NE). The increase in thermo-mechanical properties suggested the existence of strong interaction between GNPs and the epoxy network. The fracture toughness (K_{IC}) of the nanocomposites increased up to ~ 63% compared to the NE system. The fracture surfaces revealed the existence of strong covalent bonding between amine-functionalized GNPs and the epoxy network. The suggested two-step process can exhibit an inordinate potential to replace the costly multistep oxidation methods of fabrication of graphene/epoxy nanocomposites.

CRediT authorship contribution statement

Nazrul Islam Khan: Data curation, Writing - original draft, Conceptualization, Methodology. **Sudipta Halder:** Supervision, Funding acquisition, Writing - review & editing. **Nabajyoti Talukdar:** Visualization, Investigation. **Subhankar Das:** Methodology, Project administration, Characterization. **M.S. Goyat:** Project administration, Funding acquisition, Writing - review & editing.

Declaration of competing interest

The authors declare that they have no known competing financial interests or personal relationships that could have appeared to influence the work reported in this paper.

Acknowledgements

This work was financially supported by the Science and Engineering Research Board, Department of Science & Technology, Government of India (Empowerment and Equity Opportunities for Excellence in Science with Grant No. EEQ/2018/001101). The authors thank the Department of Science and Technology, India under DST-FIST program 2014 (Grant No. SR/FST/ETI-373/2014).

References

[1] K.S. Novoselov, A.K. Geim, S. V Morozov, D. Jiang, Y. Zhang, S. V Dubonos, I. V Grigorieva, a a Firsov, Electric field effect in atomically thin carbon films, Science 306 (2004) 666–669.
[2] M.J. Allen, V.C. Tung, R.B. Kaner, Honeycomb Carbon : a review of graphene, Chem. Rev. (2010) 132–145.
[3] R.J. Young, I.A. Kinloch, L. Gong, K.S. Novoselov, The mechanics of graphene nanocomposites: a review, Compos. Sci. Technol. 72 (2012) 1459–1476.
[4] L.C. Hollaway, A review of the present and future utilisation of FRP composites in the civil infrastructure with reference to their important in-service properties, Construct. Build. Mater. 24 (2010) 2419–2445.
[5] A. Journal, Y. Tong, S. Bohm, M. Song, Graphene based materials and their composites as coatings, Austin J. Nanomed. Nanotechnol. 1 (2013) 1–16.
[6] T. Kuilla, S. Bhadra, D. Yao, N. Hoon, S. Bose, J. Hee, Recent advances in graphene based polymer composites, Prog. Polym. Sci. 35 (2010) 1350–1375.
[7] V. Dhand, K.Y. Rhee, H.J. Kim, D.H. Jung, A comprehensive review of graphene Nanocomposites : research status and trends, J. Nanomater. 2017 (2013) 1–14.
[8] A. Hussain, S.M. Mehdi, N. Abbas, M. Hussain, R.A. Naqvi, Synthesis of graphene from solid carbon sources: a focused review, Mater. Chem. Phys. 248 (2020) 122924.
[9] Y. Zhu, S. Murali, W. Cai, X. Li, J.W. Suk, J.R. Potts, R.S. Ruoff, Graphene and graphene oxide: synthesis, properties, and applications, Adv. Mater. 22 (2010) 3906–3924.
[10] J.R. Potts, D.R. Dreyer, C.W. Bielawski, R.S. Ruoff, Graphene-based Polymer Nanocomposites, 2011, p. 52, https://doi.org/10.1016/j.polymer.2010.11.042.
[11] W. Choi, I. Lahiri, R. Seelaboyina, Y.S. Kang, Synthesis of graphene and its applications: a review, Crit. Rev. Solid State Mater. Sci. 35 (2010) 52–71.
[12] W.K. Chee, H.N. Lim, N.M. Huang, I. Harrison, Nanocomposites of graphene/polymers: a review, RSC Adv. 5 (2015) 68014–68051.
[13] B. Shen, W. Zhai, M. Tao, D. Lu, W. Zheng, Chemical functionalization of graphene oxide toward the tailoring of the interface in polymer composites, Compos. Sci. Technol. 77 (2013) 87–94.
[14] S. Stankovich, R.D. Piner, S.B.T. Nguyen, R.S. Ruoff, Synthesis and exfoliation of isocyanate-treated graphene oxide nanoplatelets, Carbon N. Y. 44 (2006) 3342–3347.
[15] D. V Talapin, Y. Yin, Themed issue: chemical transformations of nanoparticles, J. Mater. Chem. 21 (2011) 11454–11456.
[16] Z. Li, R.J. Young, R. Wang, F. Yang, L. Hao, W. Jiao, W. Liu, The role of functional groups on graphene oxide in epoxy nanocomposites, Polymer 54 (2013) 5821–5829.
[17] Q. Jing, W. Liu, Y. Pan, V.V. Silberschmidt, L. Li, Z.L. Dong, Chemical functionalization of graphene oxide for improving mechanical and thermal properties of polyurethane composites, Mater. Des. 85 (2015) 808–814.
[18] Nazrul Islam Khan, Sudipta Halder, Jialai Wang, Diles-Alder based epoxy matrix and interfacial healing of bismaleimide grafted GNp infused hubrid nanocomposites, Polym. Test. 74 (2019) 138–151.
[19] A. Polymer, M. Group, A. Polymer, M. Group, A. Polymer, M. Group, Graphene oxide functionalization with silanes for advanced compatibility in epoxy nanocomposites 78 (2016) 79–88.
[20] Y.J. Wan, L.X. Gong, L.C. Tang, L.B. Wu, J.X. Jiang, Mechanical properties of epoxy composites filled with silane-functionalized graphene oxide 64 (2014) 79–89.
[21] J. Wang, C. Xu, H. Hu, L. Wan, R. Chen, H. Zheng, F. Liu, M. Zhang, X. Shang, X. Wang, Synthesis, mechanical, and barrier properties of LDPE/graphene nanocomposites using vinyl triethoxysilane as a coupling agent, J. Nanoparticle Res. 13 (2011) 869–878.
[22] W. Li, B. Zhou, M. Wang, Z. Li, R. Ren, Silane functionalization of graphene oxide and its use as a reinforcement in bismaleimide composites, J. Mater. Sci. 50 (2015) 135496021.
[23] X. Yang, X. Wang, J. Yang, J. Li, L. Wan, Functionalization of graphene using trimethoxysilanes and its reinforcement on polypropylene nanocomposites, Chem. Phys. Lett. 570 (2013) 125–131.
[24] M. Melucci, E. Treossi, L. Ortolani, G. Giambastiani, V. Morandi, P. Klar, C. Casiraghi, P. Samorì, V. Palermo, Facile covalent functionalization of graphene oxide using microwaves: bottom-up development of functional graphitic materials, J. Mater. Chem. 20 (2010) 9052–9060.
[25] J. Lin, P. Zhang, C. Zheng, X. Wu, T. Mao, M. Zhu, H. Wang, D. Feng, S. Qian, X. Cai, Reduced silanized graphene oxide/epoxy-polyurethane composites with enhanced thermal and mechanical properties, Appl. Surf. Sci. 316 (2014) 114–123.
[26] H. Yang, F. Li, C. Shan, D. Han, Q. Zhang, L. Niu, A. Ivaska, Covalent functionalization of chemically converted graphene sheets via silane and its reinforcement, Journal of Materials Cheistry 19 (2009) 4632–4638.
[27] Z. Li, R. Wang, R.J. Young, L. Deng, F. Yang, L. Hao, W. Jiao, W. Liu, Control of the functionality of graphene oxide for its application in epoxy nanocomposites, Polym. (United Kingdom). 54 (2013) 6437–6446.
[28] D.S. Kim, V. Dhand, K.Y. Rhee, S. Park, Study on the effect of silanization and improvement in the tensile behavior of graphene-chitosan-composite, Polymer (2015) 527–551.
[29] R. Moriche, A. Jim Enez-Su Arez, S.G. Prolongo, A. Ure, Electrically conductive functionalized-GNP/epoxy based composites: from nanocomposite to multiscale glass fibre composite material, Compos. Part B. 98 (2016) 49–55.
[30] X. Zhang, X. Fan, C. Yan, H. Li, Y. Zhu, X. Li, L. Yu, Interfacial microstructure and properties of carbon fiber composites modified with graphene oxide, ACS Appl. Mater. Interfaces 4 (2012) 1543–1552.
[31] X. Wang, W. Xing, P. Zhang, L. Song, H. Yang, Y. Hu, Covalent functionalization of graphene with organosilane and its use as a reinforcement in epoxy composites, Compos. Sci. Technol. 72 (2012) 737–743.
[32] Y. Ni, L. Chen, K. Teng, J. Shi, X. Qian, Z. Xu, X. Tian, C. Hu, M. Ma, Superior mechanical properties of epoxy composites reinforced by 3D interconnected graphene skeleton, ACS Appl. Mater. Interfaces 7 (2015) 11583–11591.
[33] M. Sharafimasooleh, S. Shadlou, F. Taheri, Effect of functionalization of graphene nanoplatelets on the mechanical response of graphene/epoxy composites, Mater. Des. 66 (2015) 142–149.
[34] C. Liu, G. Hu, Effect of nitric acid treatment on the preparation of graphene, Ind. Eng. Chem. Res. 53 (2014) 14310–14314.
[35] M.A. Al-Saleh, A.A. Yussuf, S. Al-Enezi, R. Kazemi, M.U. Wahit, T. Ai-Shammari, A. Al-Banna, Polypropylene/graphene nanocomposites: effects of GNP loading and compatibilizers on the mechanical and thermal properties, Materials 12 (2019) 3924.
[36] B. Li, E. Olson, A. Perugini, W.H. Zhong, Simultaneous enhancements in damping and static dissipation capability of polyetherimide composites with organosilane surface modified graphene nanoplatelets, Polymer 52 (2011) 5606–5614.
[37] G. Zhang, F. Wang, J. Dai, Z. Huang, Effect of functionalization of graphene nanoplatelets on the mechanical and thermal properties of silicone rubber composites, Materials 9 (2016) 92.
[38] N.I. Khan, S. Halder, S. Das, J. Wang, Exfoliation level of aggregated graphitic nanoplatelets by oxidation followed by silanization on controlling mechanical and nanomechanical performance of hybrid CFRP composites, Compos. B Eng. 173 (2019) 106855.
[39] S. Das, S. Halder, K. Kumar, A comprehensive study on step-wise surface modification of C60: effect of oxidation and silanization on dynamic mechanical and thermal stability of epoxy nanocomposite, Mater. Chem. Phys. 179 (2016) 120–128.
[40] M.W. Marshall, S. Popa-Nita, J.G. Shapter, Measurement of functionalised carbon nanotube carboxylic acid groups using a simple chemical process, Carbon N. Y. 44 (2006) 1137–1141.

[41] M.A. Hamon, H. Hu, P. Bhowmik, S. Niyogi, B. Zhao, M.E. Itkis, R.C. Haddon, End-group and defect analysis of soluble single-walled carbon nanotubes, Chem. Phys. Lett. 347 (2001) 8–12.
[42] S. Das, S. Halder, N.I. Khan, B. Paul, M.S. Goyat, Assessing damage mitigation by silanized milled graphite nanoparticles in hybrid GFRP laminated composites, Compos. Part A Appl. Sci. Manuf. 132 (2020).
[43] S. Berciaud, S. Ryu, L. Brus, T. Heinz, Probing the intrinsic properties of exfoliated graphene: Raman spectroscopy of free-standing monolayers, Nano Lett. (2008) 346–352.
[44] J.M. Englert, C. Dotzer, G. Yang, M. Schmid, C. Papp, J.M. Gottfried, H.-P. Steinrück, E. Spiecker, F. Hauke, A. Hirsch, Covalent bulk functionalization of graphene, Nat. Chem. 3 (2011) 279–286.
[45] N. Roy, R. Sengupta, A.K. Bhowmick, Modifications of carbon for polymer composites and nanocomposites, Prog. Polym. Sci. 37 (2012) 781–819.
[46] P.C. Ma, J.-K. Kim, B.Z. Tang, Functionalization of carbon nanotubes using a silane coupling agent, Carbon N. Y. 44 (2006) 3232–3238.
[47] C. Yeong, J. Bae, T. Kim, S. Chang, S. Young, Using silane-functionalized graphene oxides for enhancing the interfacial bonding strength of carbon/epoxy composites, Composites Part A 75 (2015) 11–17.
[48] J.K. Lee, S. Song, B. Kim, Functionalized graphene sheets-epoxy based nanocomposite for cryotank composite application, Polym. Compos. 33 (2012) 1263–1273.
[49] Y.J. Wan, L.X. Gong, L.C. Tang, L. Bin Wu, J.X. Jiang, Mechanical properties of epoxy composites filled with silane-functionalized graphene oxide, Compos. Part A Appl. Sci. Manuf. 64 (2014) 79–89.
[50] E. Donth, The size of cooperatively rearranging regions at the glass transition, J. Non-Cryst. Solids 53 (1982) 325–330.
[51] D. Vennerberg, R. Hall, M.R. Kessler, Supercritical carbon dioxide-assisted silanization of multi-walled carbon nanotubes and their effect on the thermo-mechanical properties of epoxy nanocomposites, Polymer 55 (2014) 4156–4163.
[52] K.W. Putz, M.J. Palmeri, R.B. Cohn, R. Andrews, L.C. Brinson, Effect of Cross-Link Density on Interphase Creation in Polymer Nanocomposites Effect of Cross-Link Density on Interphase Creation in Polymer Nanocomposites, 2008, pp. 6752–6756.
[53] S. Das, S. Halder, J. Wang, M.S. Goyat, A. Anil Kumar, Y. Fang, Amending the thermo-mechanical response and mechanical properties of epoxy composites with silanized chopped carbon fibers, Compos. Part A Appl. Sci. Manuf. 102 (2017) 347–356.